NANO LETTERS

pubs.acs.org/NanoLett

Influence of Particle−Substrate Interaction on Localized Plasmon Resonances

Kristy C. Vernon,*,† Alison M. Funston,‡,§ Carolina Novo,† Daniel E. Gómez,† Paul Mulvaney,‡ and Timothy J. Davis†

†CSIRO, Materials Science and Engineering and Future Manufacturing Flagship, Private Bag 33, Clayton, VIC 3168, Australia, and ‡Bio21 Institute and School of Chemistry, The University of Melbourne, Parkville, VIC 3010, Australia

ABSTRACT We present a theory for determining the localized surface plasmon resonance shifts of arbitrarily shaped metal nanoparticles on a substrate. Using a pseudoparticle concept, an expression for the particle−substrate interaction is derived, providing both physical insight and formulas to estimate the shifted plasmon resonance. The theory is verified against measured scattering spectra of nanorods on substrates. Simple formulas are provided to calculate the resonance of nanorods, spheres, and ellipsoids on dielectric substrate.

KEYWORDS Surface plasmon, nanoparticle, effective permittivity, nanorod, substrate

Localized surface plasmon resonances (LSPRs) are associated with the collective oscillations of the conduction electrons of a metallic nanoparticle. The LSPR results in strong near-fields around the particle, which are of interest in a variety of applications such as sensing, nanooptical circuitry, and solar cells.[1−13] The first experiments on LSPR date back to Faraday and his study of the colors of colloidal metallic nanoparticles.[14] Since then, chemical techniques have been developed to fabricate a variety of particle shapes, from the sphere, to ellipsoids, triangular prisms, decahedra, nanoshells, nanorice, cubes, and nanorods.[15−19] It has been shown that the wavelength of the LSPR is highly dependent on the particle shape and the surrounding environment.[8,10,13,18−20]

Knowing the wavelength of the LSPR is important for designing plasmonic systems. To measure the position of the LSPR for different particle shapes, correlation techniques have been developed that allow one to correlate the particle shape with its scattering spectrum.[21−24] One such technique is the focused ion beam registration method, which we have used in the experimental verification of our theory. In this technique, focused ion beam milling provides registration marks to locate the individual nanoparticles and to correlate electron microscope images with the spectral data.[18,24]

In single-particle measurements and in many applications of LSPR,[7,8,11,12] the nanoparticles are supported by substrates. Since the LSPR frequencies of the metallic nanoparticles are sensitive to the electric permittivity of the surrounding medium, these resonances are also affected by the presence of the substrate. The extent to which the LSPR is affected depends on the strength of the interaction with the substrate which, in turn, depends on the shape of the nanoparticle.[19] A full numerical solution of Maxwell's equations will provide the shifted LSPR,[25] and many numerical techniques are available such as finite-difference time-domain, finite element modeling, discrete dipole approximation, and boundary element modeling. However, numerical methods provide little insight into the physical mechanisms underlying the particle−substrate interaction.

The effect of the substrate on spheres and ellipsoids has been derived from first principles using the concept of the image charge.[13,26,27] However, a general theory for arbitrarily shaped particles has not been developed. In this paper we use the electrostatic eigenmode method for calculating the changes in LSPR wavelengths that arise from particle−substrate interactions for particles of arbitrary shape. We also provide simple formulas for estimating the shifted LSPR without requiring intensive numerical calculations. We will show that it is possible to replace the particle on a substrate problem with a particle in a homogeneous medium (see Figure 1) leading to an effective background permittivity. This effective permittivity is mode-dependent so that it changes depending on the LSPRs. This is useful because, unlike traditional effective background permittivities, this new model is capable of predicting mode splitting. Since the theory is analytical in nature, we are also able to identify the mechanisms and strengths of the particle−substrate interaction, which are necessary for the proper design of materials, films, and sensors that utilize the optical properties of nanoparticles.

In the electrostatic eigenmode method, the LSPRs of a metallic nanoparticle are represented by surface charge oscillations on the particle coupled with their electric fields.[28−30] The electric fields from the surface charges polarize the substrate and induce additional surface charges

* To whom correspondence should be addressed, Kristy.Vernon@csiro.au.

§ Current address: School of Chemistry, Monash University, Clayton, Victoria, 3800 Australia.

Received for review: 02/3/2010
Published on Web: 05/17/2010

DOI: 10.1021/nl100423z | *Nano Lett.* **2010,** *10,* 2080–2086

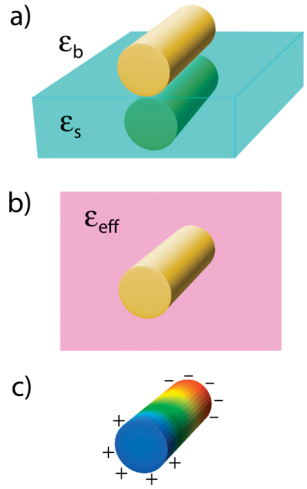

FIGURE 1. Illustration of the problem. (a) The particle on a substrate and its mirror image that acts as a pseudoparticle, where ε_b is the dielectric permittivity of the surrounding environment and ε_s is that of the substrate. According to the method discussed in this paper, this system can be mapped into (b) a particle in a homogeneous medium of permittivity ε_{eff}. (c) The surface charges of a nanorod with a predominantly dipolar mode.

at the interface between the substrate and the surrounding medium. In the case of a planar substrate, the electric field from the surface charges can be modeled using the method of images.[13,26,27,31] In this method, a surface charge $\sigma(\vec{r})$ at position $\vec{r}$ induces a surface charge $\sigma(\vec{r}_I) = [(\varepsilon_b - \varepsilon_s)/(\varepsilon_b + \varepsilon_s)]\sigma(\vec{r})$ at the mirror position $\vec{r}_I$, where ε_s is the electric permittivity of the substrate and ε_b is that of the background medium (Figure 1a). The electric field from this mirror charge then interacts with the nanoparticle leading to a shift in the frequency of the LSPR. The problem is to determine the self-consistent arrangements of charges on the nanoparticle taking into account the mirror charges.

The mirror image of the nanoparticle can be considered as a pseudoparticle that interacts with the nanoparticle (Figure 1a). This simplifies the problem and allows one to use the recently developed theory of Davis et al.[30,32] for the coupling between nanoparticles supporting LSPRs—the "electrostatic" coupling theory. In the situation where the nanoparticles are much smaller than the wavelength of the incident light, the interaction between nanoparticles is predominantly through the electric fields and Maxwell's equations take the same form as in electrostatics (even though the fields are oscillating in time at the frequency of light). The "electrostatic" coupling theory involves the eigenfunctions, or resonant modes of the nanoparticles and is applicable to nanoparticles of any shape. In this theory, the excitation amplitude a_q^k of the kth resonance mode of nanoparticle q is given by[30]

$$a_q^k(\omega) = \frac{2\gamma_q^k\varepsilon_b(\varepsilon(\omega) - \varepsilon_b)}{\varepsilon_b(\gamma_q^k + 1) + \varepsilon(\omega)(\gamma_q^k - 1)}\vec{p}_q^k\cdot\vec{E} \qquad (1)$$

where ω is the frequency of the incident light, with an electric field of amplitude $\vec{E}$, which is assumed to be uniform over the surface of the nanoparticle. The resonance is determined by the eigenvalue γ_q^k, the electric permittivity of the nanoparticle $\varepsilon(\omega)$, and the permittivity of the surrounding medium ε_b, which is taken to be real. The excitation amplitude depends on the average dipole moment $\vec{p}_q^k$ of the resonance mode. Note that these equations are applicable to any type of nanoparticle, although here we are concerned primarily with metallic nanoparticles, which exhibit strong resonances when the denominator in eq 1 is small. The average dipole moment is related to the surface normal $\hat{n}$ and to the surface dipole distribution $\tau_q^k(\vec{r})$, which is one of the two eigenfunctions obtained as solutions to the electrostatic eigenvalue problem, averaged over the surface of the nanoparticle: $\vec{p}_q^k = \oint\tau_q^k(\vec{r})\hat{n}\,dS$. The nanoparticle resonates at a frequency ω_k such that the real part of the denominator of eq 1 is zero

$$\mathcal{R}\varepsilon(\omega_k) = -\varepsilon_b\left(\frac{\gamma_q^k + 1}{\gamma_q^k - 1}\right) \qquad (2)$$

Using the pseudoparticle concept, we can represent the effect of the substrate by the electrostatic interaction of the nanoparticle with the pseudoparticle image charge. This modifies the excitation amplitude which, based on the coupling theory of Davis et al.,[30] is given by

$$\tilde{a}_q^k(\omega) = \left(\frac{2\gamma_q^k\varepsilon_b(\varepsilon(\omega) - \varepsilon_b)}{\varepsilon_b(\gamma_q^k + 1) + \varepsilon(\omega_k)(\gamma_q^k - 1) - (\varepsilon(\omega) - \varepsilon_b)\eta T_q^k}\right)\vec{p}_q^k\cdot\vec{E} \qquad (3)$$

where

$$\eta = \left(\frac{\varepsilon_b - \varepsilon_s}{\varepsilon_b + \varepsilon_s}\right) \qquad (4)$$

The modified resonance amplitude involves an extra factor T_q^k given by

$$T_q^k = \frac{\gamma_q^k}{2\pi}\oint\oint\tau_q^k(\vec{r})\frac{\hat{n}\cdot(\vec{r} - \vec{r}_I)}{|\vec{r} - \vec{r}_I|^3}\sigma_q^k(\vec{r}_I)\,dS\,dS_I \qquad (5)$$

that depends on the surface−dipole eigenfunction $\tau_q^k(\vec{r})$ of the nanoparticle and the corresponding surface-charge eigenfunction $\sigma_q^k(\vec{r}_I)$ of the nanoparticle placed at the image

DOI: 10.1021/nl100423z | *Nano Lett.* **2010,** *10,* 2080–2086

position (see Supporting Information for a full derivation). This equation involves the interaction of the electric field from the image charge with the surface dipoles on the nanoparticle. It is clear from eqs 3−5 that the resonance of the nanoparticle is altered because of its interaction with the substrate. The resonance condition can be cast into the same form as eq 2 if we define an effective background permittivity according to

$$\varepsilon_{\text{eff}} = \varepsilon_b\left(\frac{1 + \eta T_q^{\,k}/(1 + \gamma_q^{\,k})}{1 + \eta T_q^{\,k}/(1 - \gamma_q^{\,k})}\right) \tag{6}$$

such that the real part of the denominator in eq 3 is zero. Note that the resonance amplitude is not properly given by this substitution—only the position of the resonance is corrected. By defining ε_{eff}, we have taken the problem of the particle lying on a substrate and replaced it with a particle immersed in a homogeneous medium of permittivity ε_{eff}, as depicted in Figure 1. Equation 6 is useful for calculating the scattering spectra and resonances of a nanoparticle on a substrate by replacing the substrate with an effective medium.

As an alternative, it is possible to find the resonant frequency ω_S of the nanoparticle on a substrate in a medium ε_b if the resonant frequency ω_R has been found for the nanoparticle in some background medium ε_R. The formula in this case is found by combining eq 2 with eq 6 with the result

$$\mathscr{R}\varepsilon(\omega_S) = \mathscr{R}\varepsilon(\omega_R)\left(\frac{\varepsilon_b}{\varepsilon_R}\right)\left(\frac{1 + \eta T_q^{\,k}/(1 + \gamma_q^{\,k})}{1 + \eta T_q^{\,k}/(1 - \gamma_q^{\,k})}\right) \tag{7}$$

This is very similar to the formula for the effective permittivity. To find ω_S we need to know the frequency or wavelength dependence of the electric permittivity of the nanoparticle. We should point out that eq 7 is particularly useful if the resonance wavelength of the particle of interest in a homogeneous medium is known. For example, if the resonance of a nanoparticle in water has been determined, its resonance when on a substrate is easily calculated via eq 7 when the quantities γ and T are known.

The interactions of the nanoparticle with the substrate are contained in the factor $T_q^{\,k}$ which describes the effect of the electric field from the image charge on the LSPR of the nanoparticle. Both the correction formulas eqs 6 and 7 and the T-factor depend on the eigenvalue $\gamma_q^{\,k}$ that varies with the shape of the nanoparticle. Therefore, the interaction with the substrate depends on the shape of the nanoparticle and, in particular, on the aspect ratio. Moreover, we expect a dependence on the orientation of the charge distributions of the resonant mode with respect to the substrate. This can be shown explicitly using a series expansion of the term $|\vec{r} - \vec{r}_i|^{-3}$ in eq 5 which leads to an approximate form for $T_q^{\,k}$ given by

$$T_q^{\,k} \approx \frac{\gamma_q^{\,k}}{2\pi d^3}(3(\vec{p}_q^{\,k}\cdot\hat{d})^2 - \vec{p}_q^{\,k}\cdot\vec{p}_q^{\,k}) \tag{8}$$

Here d is the distance from the center of the nanoparticle to its image in the substrate, $\hat{d}$ is the unit vector pointing from the image to the nanoparticle, which is parallel to the surface normal to the substrate, and $\vec{p}_q^{\,k}$ is proportional to the dipole moment of the resonant mode k. Although this formula is very approximate, it demonstrates the orientation dependence of the T-factor through the well-known dipole−dipole interaction formula.

The effective background permittivity formulas, eqs 6 and 7, are applicable to particles of any shape and can be used for any particle−substrate system if the values of $\gamma_q^{\,k}$, $T_q^{\,k}$, ε_b, and ε_s are known. The theory can also be extended to an arbitrary number of particles on a substrate and to any number of resonant modes (see Supporting Information). In particular, for nanoparticles with multiple degenerate modes that only couple with their own image (that is, there is no cross coupling between the resonant modes), the effective permittivity formulas apply to each mode separately. Importantly, because of the orientation dependence implicit in $T_q^{\,k}$ the correction formula predicts the splitting of degenerate modes in the presence of a substrate. Details and examples are given in the Supporting Information.

Although the eigenvalue $\gamma_q^{\,k}$ is not widely used, it is directly related to the more common depolarisation factor, L. This can be seen by comparing eq 1 to the polarizability of an ellipsoid which follows from the Mie solution[26]

$$\alpha(\omega) = \varepsilon_0\left(\frac{\varepsilon(\omega) - \varepsilon_b}{\varepsilon_b + (\varepsilon(\omega) - \varepsilon_b)L}\right)V \tag{9}$$

where V is the volume of the particle. This solution is only valid for the fundamental dipole mode and is highly dependent upon the shape of the ellipsoid, which is accounted for by the depolarization factor L. The fundamental dipolar LSPR of the ellipsoid occurs at a frequency where the denominator of $\alpha(\omega)$ goes to zero, which gives the well-known condition

$$\varepsilon(\omega) = -\left(\frac{1 - L}{L}\right) \tag{10}$$

Unlike eq 9, eq 1 was derived using the electrostatic eigenvalue method and is applicable to any particle shape, which is accounted for through the eigenvalue $\gamma_q^{\,k}$. If the

DOI: 10.1021/nl100423z | Nano Lett. 2010, 10, 2080--2086

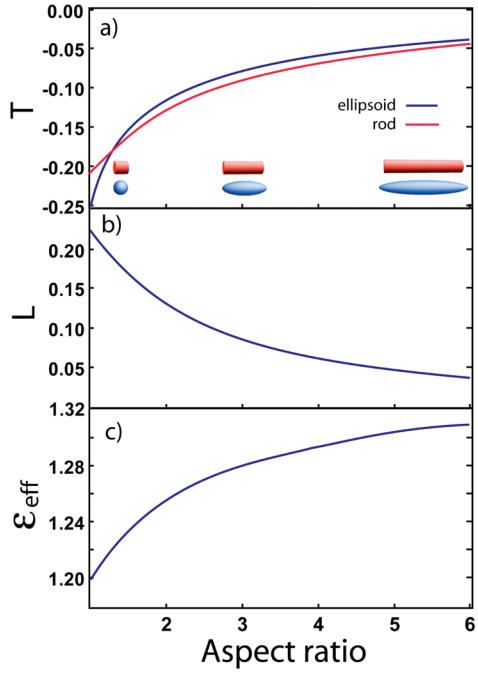

FIGURE 2. (a) The *T* integral versus aspect ratio for ellipsoids (blue) and rods (red). A sphere is an ellipsoid of aspect ratio 1. (b) The depolarization factor for rods as a function of aspect ratio and (c) the effective permittivity as a function of aspect ratio for gold nanorods in air on an ITO substrate.

predominant resonance of the particle q is dipolar, such as in the case of small prisms, rods, and ellipsoids, then the depolarization factor of this particle can be approximated from eq 10. On comparison of eq 10 to eq 2, it is clear that the depolarization factor is related to the eigenvalue γ_q^k according to

$$L = \frac{\gamma_q^k - 1}{2\gamma_q^k} \tag{11}$$

If particle q is spherical, then $\gamma_q^k = 3$ and using eq 11 we find that $L = 1/3$ as expected. The depolarization factor has been linked to the effective permittivity of the substrate for particular particle shapes,[13,18,27] but here we have a simple expression for ε_{eff} that is applicable for any particle shape, substrate, or surrounding medium. If T_q^k and L (or γ_q^k) are known for the particle of interest, then ε_{eff} can be calculated.

The values of T have been obtained for ellipsoids and are plotted in Figure 2 as a function of aspect ratio. For these calculations, the ellipsoid diameter was kept constant ($a = b$), and the length (c) was increased to give ellipsoids of different aspect ratios. The value of T was determined for the longitudinal dipole mode of the particle. As can be observed from Figure 2, as the aspect ratio of the ellipsoid increases, the interaction T with the substrate decreases. This is due to the fact that as the aspect ratio increases, the surface charges tend to remain clustered at the ends of the ellipsoid so that the fraction of the total area that interacts with the substrate decreases, and this is reflected in the value of T. As we show below, this appears counterintuitive because the effective permittivity actually increases with increasing aspect ratio.

To demonstrate the applicability of this method to shapes other than spheres and ellipsoids, we have determined the optical resonances of a nanorod using ε_{eff} and compared the results with experiments. The rods were approximated as cylinders, and the LSPR for the fundamental dipole mode (Figure 1c) were determined for different aspect ratios. The depolarization factors were determined using the electrostatic theory which yields the eigenvalue γ_q^k as a function of the aspect ratio. The depolarization factors L were then obtained using eq 11 and are shown in Figure 2b. The depolarization factor decreases with increasing aspect ratio, resulting in a larger polarizability (eq 9). This is expected, since the longer the nanorod, the more needle-like it becomes, increasing its polarizability and dipole resonance.

The value of T for the interaction of a rod with a planar substrate was also determined from eq 5 using the eigenfunctions obtained from the electrostatic calculation. Rods of aspect ratio 1−6 were modeled, and the T value compared to that of the ellipsoid (Figure 2a). The interaction of the rod with the substrate is very similar to the interaction of the ellipsoid: T decreases with increasing aspect ratio. For ease of calculation of T factors, we have formed parametric fits to these curves of the form $T = -1/(ax^2 + bx + c)$ where x is the aspect ratio. For ellipsoids we find that $a_e = -0.115$, $b_e = 4.977$, $c_e = -0.862$ and for rods $a_r = 0.181$, $b_r = 2.385$, $c_r = 2.204$. Likewise we have formed parametric fits to the eigenvalues of the form $\gamma = sx^p + k$. For the rods we have $s_r = 0.846$, $p_r = -1.132$, and $k_r = 0.965$ and for the ellipsoids we have $s_e = 1.93$, $p_e = -2.093$, and $k_e = 1.072$.

Given the values of T, the effective permittivity for the nanorod lying on an indium tin oxide (ITO)-coated glass substrate can be determined using eq 6. The results are shown in Figure 2c. The ITO permittivity was determined as a function of wavelength using spectroscopic ellipsometry and ranges from 3.13 to 2.44 for the wavelengths of interest. The ITO value used in eq 6 was chosen at the LSPR resonance determined from the electrostatic eigenvalue method (that is, from the eigenvalue γ_q^k and eq 2 assuming the nanorods were made from gold with an electric permittivity given by Johnson and Christy).[33] Although the strength of the rod−substrate interaction *decreases* as the nanorod aspect ratio is increased (that is, $|T|$ becomes smaller), the effective permittivity ε_{eff} *increases* leading to a larger shift in the LSPR position. This result agrees with the work of Myroshnychenko et al.[13] This apparent contradiction is due to the rapid change with aspect ratio of the metal permittivity $\varepsilon(\omega)$ required for resonance. The increasing aspect ratio leads to a change in γ such that $\gamma \rightarrow 1$ so that $\mathcal{R}\varepsilon(\omega)$ becomes large and negative, as given by eq 2. The changing γ

DOI: 10.1021/nl100423z | *Nano Lett.* **2010,** *10,* 2080–2086

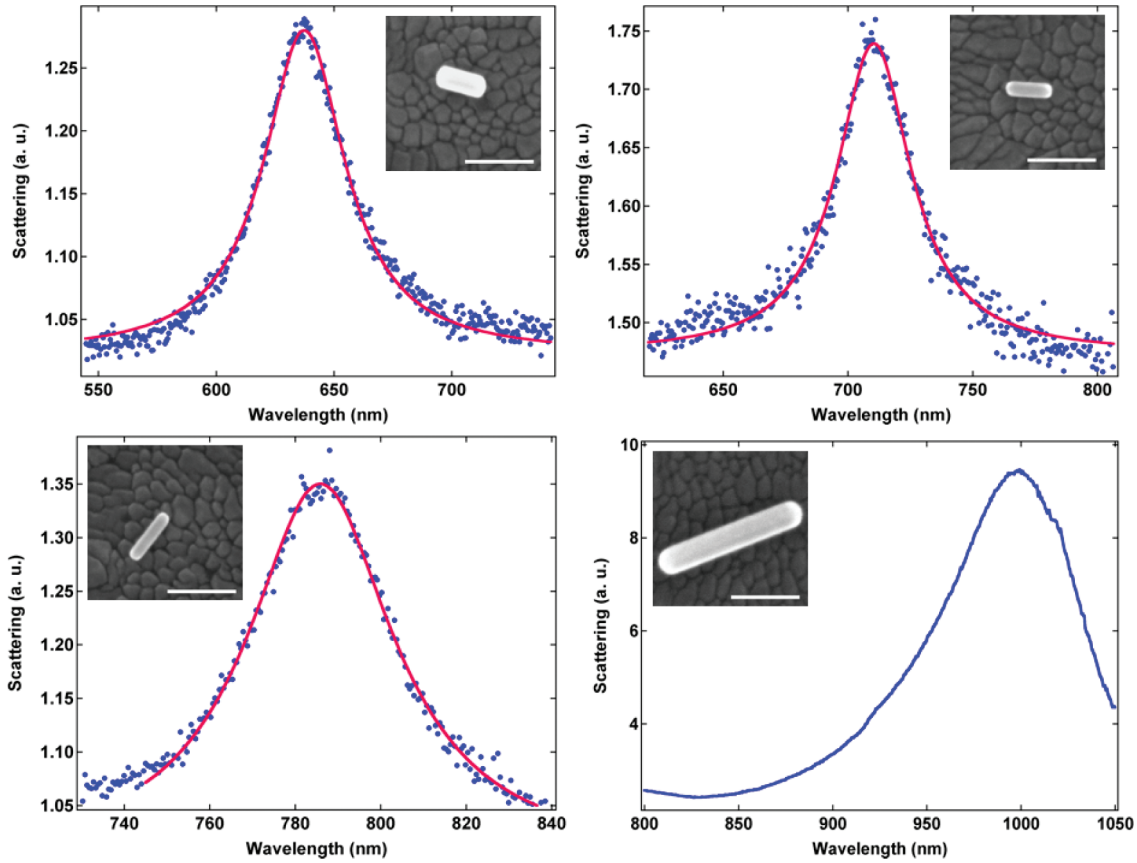

FIGURE 3. Scattering spectra and SEMs of a range of single Au nanorods with different aspect ratios on ITO-coated glass. The blue dots/line are the experimental data, the red line is a Lorentzian fit to the data. This is not included for the largest rod due to the likely contribution from higher order multipoles. Scale bars =100 nm.

counteracts the decrease in the substrate interaction resulting in the observed increase in the effective permittivity. In other words, the metal permittivity increases faster with aspect ratio than the substrate interaction decreases, leading to an overall increase in the effective permittivity.

As a test of the theory, we compare the theoretical LSPR shifts with experimentally measured values for gold nanorods. The gold nanorods were synthesized chemically using the seed-mediated growth method developed by Nikoobaht and El-Sayed.[17] For single particle spectroscopy, samples were prepared by spin coating clean, dry, ITO-coated glass slides with the diluted gold nanoparticle solution (30 μL, 3000 rpm, 5 s). The samples were allowed to dry completely before being used, leaving gold rods in air resting on the ITO substrate. The gold rods were imaged using scanning electron microscopy (SEM) (Figure 3) and registration marks were etched in the substrate to allow the correlation of the particle spectra and geometry. The rods were approximately 30 nm in diameter with lengths between 45 and 180 nm.

Spectra of individual gold nanorods were recorded using a dark field microscope. The light scattered by the single nanoparticles was collected with a Nikon Plan Fluor ELWD ×40/0.60 NA objective and detected/dispersed with a MicroSpec 2150i imaging spectrometer coupled to a TE-cooled CCD camera (PIXIS 1024B ACTON Princeton Instruments). The spectra were integrated for 60 s. The raw spectra were normalized for background light. Representative results are shown in Figure 3. The optical scattering peak positions were plotted as a function of nanorod aspect ratio (Figure 4). The observed spread in resonance wavelength is due to the polydispersity obtained in the chemical synthesis of the gold nanorods.[18] The LSPR position will vary significantly as a function of nanorod shape, specifically the shape of the endcaps, as discussed by Prescott et al. and Myroshnychenko et al.[13,34]

The theoretical curves were based on calculations of the optical scattering using COMSOL Multiphysics and are compared to the experimental results in Figure 4. The rods were modeled as gold cylinders with permittivities taken from Johnson and Christy.[33] The wavelengths associated with the LSPR were determined for the rods on the substrate using three different methods and, for comparison, two other calculations were done for homogeneous media, one of permittivity $\varepsilon_b = 1$ (air) and the other of permittivity $\varepsilon_b = 2.25$ (glass). For the substrate calculations, one set of resonances was calculated based on a homogeneous medium of ε_{eff} according to eq 6, another set was calculated

DOI: 10.1021/nl100423z | *Nano Lett.* **2010,** *10,* 2080–2086

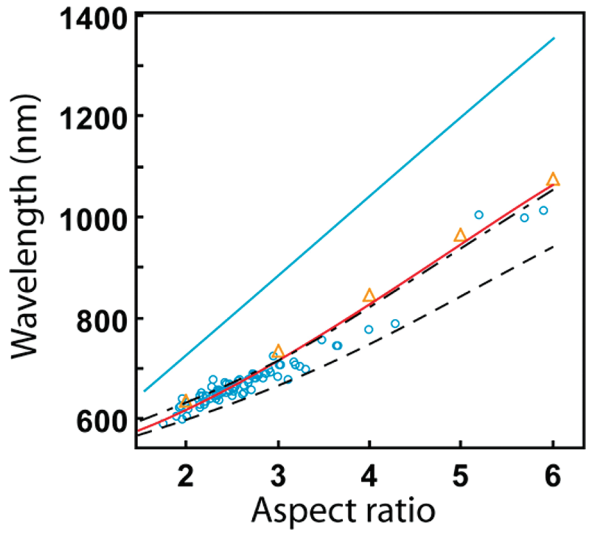

FIGURE 4. Peak scattering wavelength of single gold nanorods on ITO-coated glass as a function of aspect ratio. Experimental (circles) and predictions using a medium of permittivity 2.25 (solid blue), air (dash), the effective background permittivity (solid red), predicted shift using eq 7 (dash-dot) and full-field numerical simulations (triangles).

using the results for air and corrections to the resonances were found using eq 7, and as a further check of our theory, the scattering peaks of the rods on the substrate were determined using a full-field simulation in COMSOL Multiphysics. The results for rods in a homogeneous medium of ε_{eff} match the experimental data remarkably well across all the studied aspect ratios, considering ε_{eff} was determined using an electrostatic model which should show inaccuracies for large particles. Also, the results calculated using eq 7 based on the calculated resonances in air match the experimental data and require no numerical modeling, other than determining the resonances in air. The largest aspect ratio rod has a length of 180 nm, which is 5 times smaller than its resonance wavelength, but as recently demonstrated by Davis et al.,[35] the errors arising from the electrostatic approximation accumulate more slowly with increasing size than, for example, spheres of similar dimensions. The full-field calculations match the effective permittivity calculations and the predictions of eq 7 reasonably well with a slight red shift. The agreement between our theory and the experiment is remarkable, considering that there were no adjustable parameters in the theory. All the parameters that we used either were obtained experimentally (such as the electric permittivity of the ITO substrate), were based on the known geometry (cylinders with specified aspect ratios), or were obtained from the literature (such as the electric permittivity of gold).

In conclusion, we have developed and experimentally verified a theory for predicting the shifted LSPR of any metal nanoparticle on a substrate. This theory is applicable to particles of arbitrary shape and is derived within the electrostatic limit, implying particle sizes smaller than the optical resonance wavelength of interest.[35] The resonance of a particle on a substrate can be determined for any nanoparticle−substrate system provided that the double integral T and the depolarization factor (or eigenvalue γ) are known. We have also derived a simple formula that relates the LSPR frequency of a particle on a substrate to that of the particle in a homogeneous medium, with no adjustable parameters, and we have shown that this formula yields excellent agreement with experimental data. If the resonance wavelength of the particle in a homogeneous medium is already known, then given values for γ and T no numerical modeling is needed to estimate the resonance shifts in the presence of a substrate. We have provided values of γ and T for spherical, ellipsoidal, and cylindrical nanoparticles. Furthermore, we have derived an effective background permittivity, which, unlike conventional effective permittivities, can take into account mode-splitting, and have used the effective permittivity and numerical modeling to obtain scattering spectra of gold nanorods on an ITO substrate, verifying the predictions with experimental results. This analytical technique provides insight into the particle−substrate interaction and greatly simplifies the modeling of the particle−substrate system for predicting the LSPR shifts. Such predictions are important for the design of metallic nanoparticle systems for refractive index and biosensors. We anticipate that the theory will be useful for plasmon studies at the single particle level.

Supporting Information Available. Full derivation of eqs 6 and 7 and extended derivation to an arbitrary number of particles. This material is available free of charge via the Internet at http://pubs.acs.org.

REFERENCES AND NOTES

(1) Anker, J. N.; Hall, W. P.; Lyandres, O.; Shah, N. C.; Zhao, J.; Duyne, R. P. V. *Nat. Mater.* **2008**, *7*, 442–453.
(2) Banholzer, M. J.; Millstone, J. E.; Qin, L.; Mirkin, C. A. *Chem. Soc. Rev.* **2008**, *37*, 885–897.
(3) Brown, R. J. C.; Milton, M. J. T. *J. Raman Spectrosc.* **2008**, *39*, 1313–1326.
(4) Davis, T. J.; Vernon, K. C.; Gómez, D. E. *J. Appl. Phys.* **2009**, *106*, No. 043502.
(5) Hägglund, C.; Zäch, M.; Petersson, G.; Kasemo, B. *Appl. Phys. Lett.* **2008**, *92*, No. 053110.
(6) Jain, P. K.; El-Sayed, M. A. *Nano Lett.* **2008**, *8*, 4347–4352.
(7) Kim, S.-S.; Na, S.-I.; Jo, J.; Kim, D.-Y.; Nah, Y.-C. *Appl. Phys. Lett.* **2008**, *93*, No. 073307.
(8) Lal, S.; Link, S.; Halas, N. J. *Nat. Photonics* **2007**, *1*, 641–648.
(9) Lal, S.; Grady, N. K.; Kundu, J.; Levin, C. S.; Lassiter, J. B.; Halas, N. J. *Chem. Soc. Rev.* **2008**, *37*, 898–911.
(10) Murray, W.; Barnes, W. *Adv. Mater.* **2007**, *19*, 3771–3782.
(11) Larsson, E.; Alegret, J.; Kall, M.; Sutherland, D. *Nano Lett.* **2007**, *7*, 1256–1263.
(12) Atwater, H.; Maier, S.; Polman, A.; Dionne, J.; Sweatlock, L. *MRS Bull.* **2005**, *30*, 385–389.
(13) Myroshnychenko, V.; Rodriguez-Fernandez, J.; Pastoriza-Santos, I.; Funston, A.; Novo, C.; Mulvaney, P.; Liz-Marzan, L.; de Abajo, F. G. *Chem. Soc. Rev.* **2008**, *37*, 1792–1805.
(14) Faraday, M. *Philos. Trans. R. Soc. London* **1857**, *147*, 145.
(15) Wang, H.; Brandl, D.; Le, F.; Nordlander, P.; Halas, N. *Nano Lett.* **2006**, *6*, 827–832.
(16) Sun, Y.; Xia, Y. *Science* **2002**, *298*, 2176–2179.
(17) Nikoobaht, B.; El-Sayed, M. *Chem. Mater.* **2003**, *15*, 1957–1962.

DOI: 10.1021/nl100423z | *Nano Lett.* **2010,** *10,* 2080–2086

(18) Novo, C.; Funston, A. M.; Pastoriza-Santos, I.; Liz-Marza'n, L. M.; Mulvaney, P. *J. Phys. Chem. C* **2008**, *112*, 3–7.
(19) Haynes, C.; Van Duyne, R. *J. Phys. Chem. B* **2001**, *105*, 5599–5611.
(20) Kelly, K. L.; Coronado, E.; Zhao, L. L.; Schatz, G. C. *J. Phys. Chem. B* **2003**, *107*, 668–677.
(21) Hu, M.; Chen, J.; Marquez, M.; Xia, Y.; Hartland, G. *J. Phys. Chem. C* **2007**, *111*, 12558.
(22) Nehl, C.; Grady, N.; Goodrich, G.; Tam, F.; Halas, N.; Hafner, J. *Nano Lett.* **2004**, *4*, 2355.
(23) Billaud, P.; Marhaba, S.; Cottancin, E.; Arnaud, L.; Bachelier, G.; Bonnet, C.; Fatti, N.; Lerme, J.; Vallee, F.; Vialle, J.; Broyer, M.; Pellarin, M. *J. Phys. Chem. C* **2008**, *112*, 978.
(24) Novo, C.; Funston, A.; Pastoriza-Santos, I.; Liz-Marzan, L.; Mulvaney, P. *Angew. Chem., Int. Ed* **2007**, *46*, 3517–3520.
(25) Knight, M.; Wu, Y.; Lassiter, J. B.; Nordlander, P.; Halas, N. *Nano Lett.* **2009**, *9*, 2188–2192.
(26) Kreibig, U.; Vollmer, M. *Optical properties of metal clusters*; Springer: Berlin, 1995.
(27) Yamaguchi, T.; Yoshia, S.; Kinbara, A. *Thin Solid Films* **1974**, *21*, 173–187.
(28) Mayergoyz, I.; Fredkin, D.; Zhang, Z. *Phys. Rev. B* **2005**, *72*, 155412.
(29) Mayergoyz, I.; Zhang, Z.; Miano, G. *Phys. Rev. Lett.* **2007**, *98*, 147401.
(30) Davis, T. J.; Vernon, K. C.; Gómez, D. E. *Phys. Rev. B* **2009**, *79*, 155423.
(31) Jackson, J. *Classical Electrodynamics*; John Wiley and Sons: New York, 1962.
(32) Funston, A. M.; Novo, C.; Davis, T. J.; Mulvaney, P. *Nano Lett.* **2009**, *9*, 1651–1658.
(33) Johnson, P.; Christy, R. *Phys. Rev. B* **1972**, *6*, 4370–4379.
(34) Prescott, S.; Mulvaney, P. *J. Appl. Phys.* **2006**, *99*, 123504. Prescott, S.; Mulvaney, P. *J. Appl. Phys.* **2008**, *103*, 119901 (erratum).
(35) Davis, T. J.; Vernon, K. C.; Gómez, D. E. *Opt. Express* **2009**, *17*, 23655–23663.

DOI: 10.1021/nl100423z | *Nano Lett.* **2010,** *10,* 2080--2086